Journal of Molecular Liquids xxx (xxxx) 120893

Contents lists available at ScienceDirect

Journal of Molecular Liquids

journal homepage: www.elsevier.com/locate/molliq

The effect of temperature and external force on the thermal behavior of oil-based refrigerant inside an atomic nanochannel using molecular dynamics simulation

Haoran Cheng [a,*], Azher M. Abed [b], As'ad Alizadeh [c], Amer Ali Ghabra [d], Farag M. A. Altalbawy [e,f], Roozbeh Sabetvand [g], Ghassan Fadhil Smaisim [h,i], Anupam Yadav [j], Davood Toghraie [k], Yassine Riadi [l]

[a] Research Institute of Tsinghua University in Shenzhen, Shenzhen 518000, China
[b] Air conditioning and Refrigeration Techniques Engineering Department, Al-Mustaqbal University College, Babylon, 51001, Iraq
[c] Department of Civil Engineering, College of Engineering , Cihan University-Erbil, Erbil , Iraq
[d] Al-Amarah University College, Al-Amarah, Iraq
[e] Department of Chemistry, University College of Duba, University of Tabuk, Duba 71911, Saudi Arabia
[f] National Institute of Laser Enhanced Sciences (NILES), University of Cairo, Giza 12613, Egypt
[g] Department of Energy Engineering and Physics, Faculty of Condensed Matter Physics, Amirkabir University of Technology, Tehran, Iran
[h] Department of Mechanical Engineering, Faculty of Engineering, University of Kufa, Iraq
[i] Nanotechnology and Advanced Materials Research Unit (NAMRU), Faculty of Engineering, University of Kufa, Iraq
[j] Department of CEA, GLA University, Mathura 281406, India
[k] Department of Mechanical Engineering, Khomeinishahr Branch, Islamic Azad University, Khomeinishahr Khomeinishahr, Iran
[l] Department of Pharmaceutical Chemistry, College of Pharmacy, Prince Sattam bin Abdulaziz University, Al-Kharj 11942, Saudi Arabia

ARTICLE INFO

Article history:
Received 13 April 2022
Received in revised form 27 October 2022
Accepted 24 November 2022

Keywords:
Nanofluid (NF)
Heat transfer
Nanochannel
Heat flux
Thermal conductivity

ABSTRACT

Heat transfer (HT) has always been one of the major challenges in engineering. Many approaches have been offered to enhance or control HT. One of the common techniques to develop the thermal performance of devices is to use nano-sized channels. This study is aimed to examine the influence of temperature and external force (EF) on nanochannel simulated samples by molecular dynamics simulation (MDS). The present study examined the effect of initial temperature (300–400 K) and EF (with 0.001–0.01 eV/Å) on oil inside the nanochannel. The results show that increasing temperatures up to 350 K increases the heat flux (HF) and thermal conductivity (TC) increase and decreases due to the increased number and intensity of atomic collisions in the structures. The HF and TC at 350 K are 946 W/m^2 and 0.66 W/m.K. Also, by changing the EF from 0.001 to 0.01 eV/Å, the HF increases from 911 to 942 W/m^2 and the TC by 0.52 to 0.63 W/m.K. So, with an increment in EF, oscillation amplitude increases, and thermal performance improves. Since the thermal performance of refrigerant is noticeable in various industrial applications, it's hopeful this study proposed an optimal mechanism in practical samples.

Nomenclature

σ	potential well's depth;
ε	finite distance at which the potential becomes zero;
r_{ij}	atomic distance between i and j particles,
r_c	cut-off distance;
k_r	oscillator constant
r_0	oscillator's bond length;
k_θ	angular oscillator's constant;
θ_0	equilibrium value of the oscillator's angle;
t,	MD simulation time;

Abbreviations: MD, Molecular Dynamics; Ns, Nanosecond; eV, electron Volt; UFF, Universal Force Field; EAM, Embedded-Atom Method; LJ, Lennard-Jones; LAMMPS, large scale atomic/molecular massively parallel simulation

https://doi.org/10.1016/j.molliq.2022.120893
0167-7322/

1. Introduction

Investigating the behavior of heat transfer fluids has always been an exciting topic for researchers. Heating and heat removal from different systems or heating systems has always been among the topics researched by researchers [1–3]. One of the ways to increase the heat transfer rate is to add particles to common heat transfer fluids. These particles are usually in nano dimensions. Nanoparticles are found in various shapes and morphologies depending on their application, including spherical, tubular, and laminated structures. Refrigerant is the operating fluid used in refrigeration cycles and heat pumps. It must have desirable thermodynamic properties and processes such as non-toxicity, non-corrosiveness of mechanical equipment, non-flammability, and environmental compatibility [4]. In addition, refrigerants should not have destructive effects on the ozone layer and climate change [5]. The task of refrigerants is to receive heat from the desired environment and transfer it out of the environment. In refrigerants, the ability to alter the phase from liquid to gas and vice versa due to their performance in thermodynamic systems for heat transfer (HT) is particularly important [6–8]. Compressors of compression refrigeration cycles are used. The refrigerant must be compatible with the oil in the compressor. By adding nanoparticles (NPs), the thermal properties of oils can be improved [9]. Common methods for increasing HT include increasing the surface area of the HT surface, vibrating the surfaces or fluid being heated, and using an electric field to optimize existing HT systems by increasing their surface area by expanded surfaces such as vanes and microchannels [10–13]. Oils containing NPs are widely used in the power industry (power and transmission lines), reduce energy consumption, reduce the flow in power lines and increase thermal and electrical properties [14]. An extensive numerical and experimental investigation has been conducted on the HT of nano-refrigerants [15–19]. Ahmadpour et al. [20] examined condensation HT characteristics of R-600a/oil/MWCNT nano-refrigerant flow. This research group showed that the coefficient of HT of R-600a/oil is loftier than R-600a. The pure R-600a has a higher coefficient at high qualities since greasing up oil influences the thermal resistor of the condensed fluid film. In another study, Feng et al. [21] investigated the influence of adding NPs to an oil and how the fluid moves inside a nanochannel.

The simulation outcomes display that adding NPs to the oil in the silica nanochannel improves the fluid motion and thermophysical properties. Wang et al. [22] prepared a novel kind of diathermic oil with alumina-zinc oxide (AZO) NFs and analyzed the properties of NFs. The expansion of novel NPs compensates for the lack of DO function as HT fluid. The results show that the TC of AZO NFs was upgraded to 8.125 % compared with DO. Wu et al. [23] added nano-graphene sheets inside an oil fluid. They evaluated how many nanosheets are used inside the oil fluid, resulting in a stable structure simulated under standard conditions. Salem et al. [24] inspected the impact of MWCNT NPs on condensation HT features of R600a/oil mixture. The results showed that at slight vapour modality, augmenting greasing up oil into the refrigerant progresses the HT coefficient of the NFs. Yong et al. [25] investigated how the added NPs interacted with the oil–water fluid and performed molecular dynamics simulation (MDS) using LAMMPS software. To define the interaction between the added NPs and the oil–water fluid, the team investigated items such as the energy of the system and the density of the NPs in different parts of the fluid and reported their results. Studying the NFs' thermal properties still needs further investigation and is especially important for thermal management applications. Due to the experimental limitations, numerical simulations are used to analyze the thermal behavior inside the nanochannel. Therefore, in the present paper, the thermal behavior of the oil inside the nanochannel was examined by the MDS method. This study investigated the effect of initial temperature (300, 310, 320, 350 and 400 K) and external force (EF) (0.001, 0.002, 0.003, 0.005 and 0.01 eV/Å) on heat flux (HF) and TC.

2. Simulation

2.1. MD method

The foremost critical apparatuses to study the function of biological macromolecules and their physical structure is MDS. The MDS technique computes the time-dependent conduct of the particle system and utilizes the relations of motion to obtain the particle path. Thus, with computation of the time-dependent behavior, the system obtains information such as velocity and acceleration of particles at the nano level, which with the help of statistical approaches to these microscopic outcomes, determines the macroscopic properties of the system. MDS follows the equation of motion as follows:

$$F_i = m_i a_i \tag{1}$$

where F_i represents the force exerted on atom i in the N atomic system. Here m_i is the mass, and a_i acceleration is as follows:

$$a_i = \frac{d^2 r_i}{dt^2} \tag{2}$$

From the combination of the above relations, the position of the particles is obtained through the potential function:

$$-\frac{dU}{dr_i} = m_i \frac{d^2 r_i}{dt^2} \tag{3}$$

Analytical description of particle motion is very difficult due to the coupling nature of particle motion, and therefore it is better to coordinate the movement equation. Verlet algorithm is one of the most common methods of integrating motion equations in MDS. It is one of the most accurate and simple algorithms, in which time is reversible [26].

$$r_i\ (t - \Delta t) = r_i\ (t) - \left(\frac{dr_i}{dt}\right) \Delta t + \frac{1}{2}\left(\frac{d^2 r_i}{dt^2}\right) (\Delta t)^2 + ... \tag{4}$$

$$r_i\ (t + \Delta t) = r_i\ (t) + \left(\frac{dr_i}{dt}\right) \Delta t + \frac{1}{2}\left(\frac{d^2 r_i}{dt^2}\right) (\Delta t)^2 + ... \tag{5}$$

$$v_i(t) = \frac{r_i\ (t + \Delta t) - r_i\ (t - \Delta t)}{2\Delta t} + O(\Delta t^2) \tag{6}$$

In computer simulations, bonded and unbound forces are expressed as a set of mathematical equations and are of great importance in the accuracy of the simulation results. Consequently, the main problem is finding the interaction between atoms and the forces acting on them at any given moment. The choice of an interatomic potential, the mode of interaction of atoms, is certainly the main input for developing an atomic model. In the present work, the sum of Lennard-Jones (LJ), EAM, and Columb potential functions is used. There are many classic potentials, one of the simplest and most practical of which is the LJ potential. The potential of LJ [27] is used for non-bonding interactions and is as follows:

$$U = \sum_{i<j} 4\varepsilon \left[\left(\frac{\sigma}{R_{ij}}\right)^2 - \left(\frac{\sigma}{R_{ij}}\right)^6\right] \tag{7}$$

* Corresponding author.
E-mail address: Toghraee@iaukhsh.ac.irchen (H. Cheng).

where R_{ij} is the distance between the centers of atoms or non-bonded groups, and σ is the depth of the well of potential. The σ and ε amount of present particles are reported in Table 1.

The EAM potential is utilized to specific the interplay among metal particles, which is presented in the following relation [30]:

$$U = F_\alpha \left(\sum_{i \neq j} \rho_\beta \left(r_{ij} \right) \right) + \frac{1}{2} \sum_{i \neq j} \phi_\beta \left(r_{ij} \right) \tag{8}$$

In this relation, F_α, ρ_β, and ϕ_β are a constant coefficient between 0 and 1, the atomic charge density, and the attendance of particles in the box of simulation. Electric potential energy is acquired using Columb steady forces. This energy defines the number of static electric charge particles in a system that repels or absorbs each other. The electric potential energy is obtained from the following equation [31]:

$$U(r) = \frac{-1}{4\pi\varepsilon_0} \frac{q_i q_j}{r_{ij}^2} \tag{9}$$

where q_i and q_j are electric charges i and j, $r_{ij,}$ the distance among the charges and ε_0 represent the electrical permeability of the open space and are numerically equivalent to 8.85 × 10^{-12}F·m $^{-1}$. Two methods of equilibrium dynamics and non-equilibrium dynamics are used to study the thermal properties of MDS. Non-equilibrium simulation is usually faster but less accurate than the equilibrium method. Therefore, the alternative method to the non-equilibrium method is the equilibrium method. In equilibrium simulation, no temperature difference is applied to the system, but vibration and particle motion predictions are used to determine the temperature properties. This type of heat calculation is possible using the Green-Kubo relation, which is as follows [32]:

$$K = \frac{V}{3k_B T^2} \int_0^\infty dt \left\langle J(\tau) . J(0) \right\rangle$$

In this relation, V is the volume occupied by the particles present in the simulation, kB, T, and J are constant of Boltzmann, temperature, and the HF.

Table 1
LJ potential factors for particle atoms in MDSs [28,29].

Type of atom	ε (kcal/mol)	σ (Å)	r_c (Å)
Al	0.0650	1.140	12
O	0.1553	3.166	12
Cu	0.005	3.195	12
C	0.105	3.851	12
Fe	0.055	4.540	12

2.2. Simulation details

The current investigation will investigate the phenomenon of HT in an aluminum nanochannel by a base oil. The simulations of this study first simulate an ideal oil sample, which includes ester-based oils and hydrocast-based oils, respectively. Initial modeling was performed by Avogadro and VMD software. The present simulation was performed by LAMMPS software. Boundary conditions are fixed in the × and y-orientations and periodic in the z-direction. The simulation time in the process of balancing atomic samples is 10 ns. The time-step is 1 fs. The microcanonical ensemble has been utilized within the simulations accomplished in this investigation. The structures' thermal behavior will be done simultaneously in equilibrium (certain initial temperature). The Green-Kubo method has been used to study the thermal behavior in atomic samples, the equilibrium method, and, more precisely, Fig. 1 shows a schematic of the movement of an ester-based oil inside an aluminum nanochannel.

3. Result

Physical amounts like temperature and potential energy (PE) of the samples are investigated and reported to check the equilibrium in the simulated samples. Then the effect of initial temperature with values of 300, 310, 320, 350, and 400 K and EF with values of 0.001 eV/Å, 0.002 eV/Å, 0.003 eV/Å, 0.005 eV/Å and 0.01 eV/Å on the thermal behavior of oil in the nuclear nanochannel is investigated.

3.1. Stability process

Fig. 2 displays the temperature variations in the samples over time. Based on this diagram, the temperature value in the final structure converges to 300 K after 10 ns. This behavior occurs in the simulated samples because of the decrease of atomic fluctuations and the consequent convergence of the location of the atoms to the final and equilibrium position. This result indicates that modeling atomic structures, interatomic potentials, and MDS configurations are well done.

Fig. 3 displays the PE in simulation time. As shown in Fig. 3, evaluating potential energy in samples can also be a good criterion for reporting equilibrium behavior in atom-based samples. As time goes on, the value of potential energy in the samples converges to a negative amount. This convergence in potential energy indicates the presence of gravity in the sample and, thus, its stability. With the enhancement of this amount, it is expected that the value of stability in the samples will increase. More precisely, due to the negation of potential energy, it can be said that the sample has thermodynamic stability because of the gravitational force among particles. As this physical amount becomes more negative, the stability in the samples will increase. The PE con-

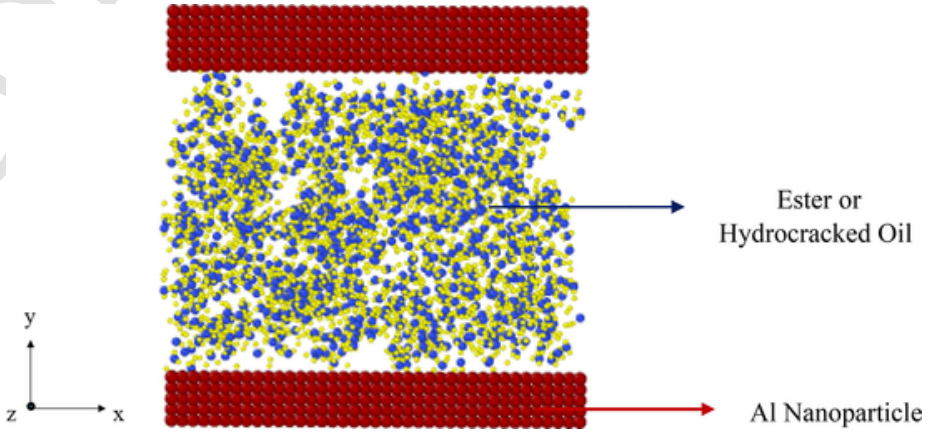

Fig. 1. Schematic the movement of an ester-based oil inside a nanochannel.

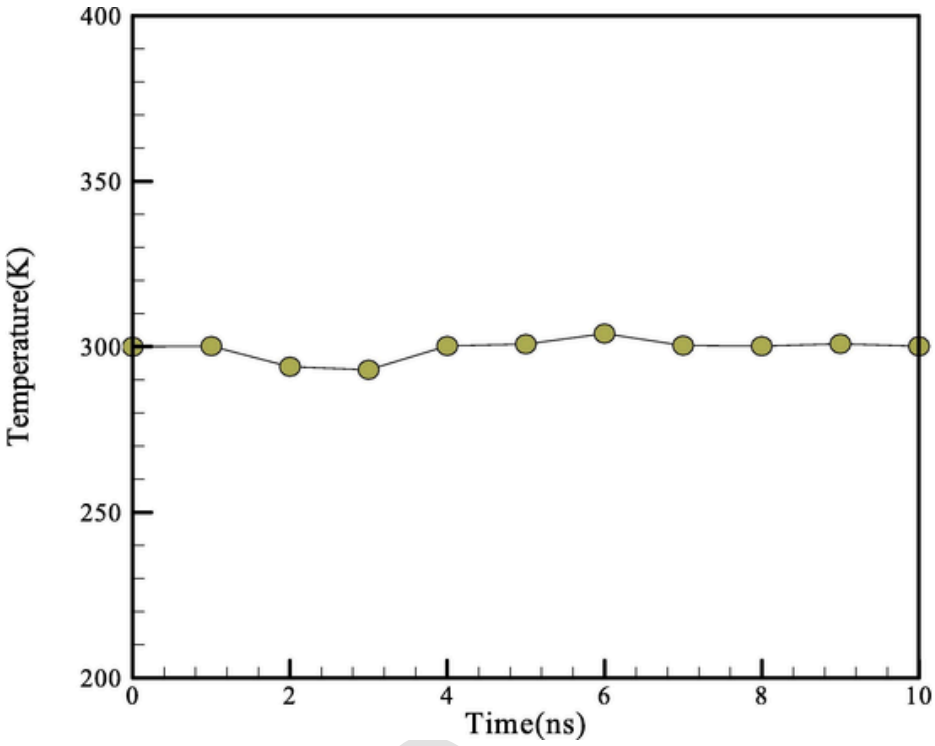

Fig. 2. Temperature variations in structures applying simulation time.

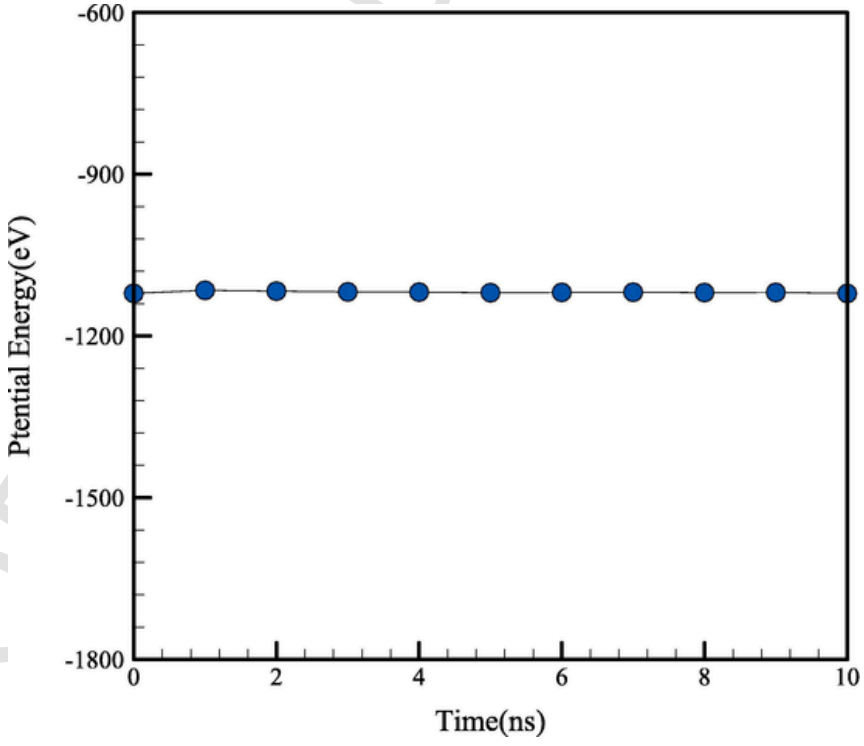

Fig. 3. Changes in PE over simulation time.

verges to −1121 eV after 10 ns. The evaluation of PE in samples can also be a good criterion for reporting equilibrium behavior in samples based on atoms.

3.2. The impact of initial temperature on the thermal manner of oil within the atomic nanochannel

A change in the initial T alters their mobility and, as a result, can alter the thermal behavior of these structures. The initial T is changed to investigate this issue. The initial temperature of these simulated samples is balanced in numerical values, including 300, 310, 320, 350, and 400 K for 10 ns, and their thermal behavior is investigated. Fig. 4 shows the changes in oil flux based on hydrocast in terms of initial temperature after 10 ns. According to Fig. 4, as the temperature increases, the thermal behavior of the simulated structures increases to 350 K and then decreases. As the structure's temperature increases and the atomic motion increases, the HT in the structures enhances. This is understandable due to the increase in the number and severity of interatomic collisions. The numerical results are reported in Table 2.

Fig. 5 shows the changes in the TC of the oil-based hydrocast according to the initial temperature after 10 ns. According to Fig. 5, as the T increases, the TC of the simulated samples increases to 350 K and then decreases. As the number and intensity of atomic collisions increase, the amount of heat transferred to the structure also increases, resulting in improved TC in atomic samples. Atomically, this is due to increased atomic motion with increasing temperature. More precisely, based on $\frac{1}{2}mv^2 = \frac{3}{2}kT$ kinetic energy (movement of atoms) and the temperature of the atomic sample are directly related to each other.

Table 2 indicates the HF and TC based on the initial temperatures in the oil sample based on hydrocast after 10 ns. According to Table 2, the maximum flux and TC at 350 K equal 946 W/m^2 and 0.66 W/m.K. The minimum flux and TC at 300 K equal 911 W/m^2 and 0.52 W/m.K. Physically, structural coherence in oil samples decreases with excessive temperature increase in atomic samples (simulated oil). To be more precise, excessive temperature increase causes excessive oscillation amplitude in atomic samples. As a result, the amount of van der Waals absorption force in the structures converges to smaller values, which will reduce the HT in these structures.

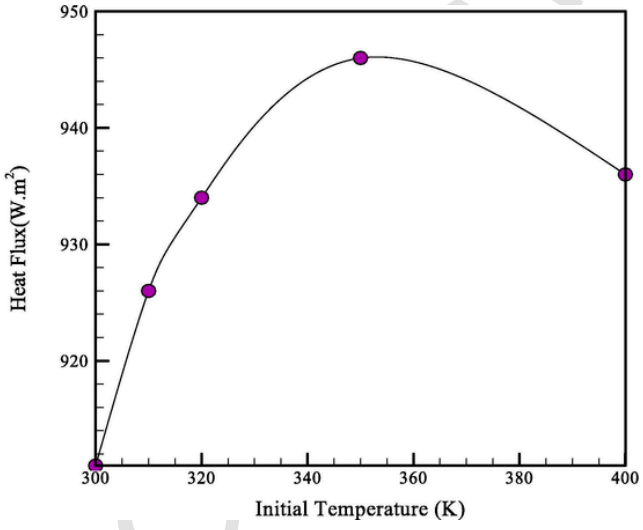

Fig. 4. Hydrocast oil-based HF changes in initial temperature after 10 ns.

Table 2
HF and TC based on initial temperatures in an oil hydrocast-based sample after 10 ns.

Initial temperature (K)	HF (W/m ^{2})	TC (W/m.K)
300	911	0.52
310	926	0.58
320	934	0.62
350	946	0.66
400	936	0.65

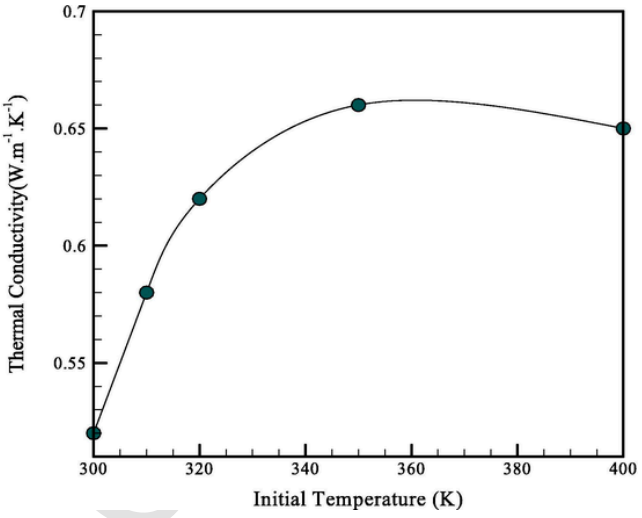

Fig. 5. Changes in TC of oil based on hydrocast according to initial temperature after 10 ns.

3.3. The influence of EF on the thermal conductivity of oil inside the atomic nanochannel

Change in the amount of EF is an influential factor in the thermal proficiency of samples. In the last part of the investigation, EF's impact on the TC of NF based on hydrocast in the attendance of 4 % NPs is investigated. For this purpose, an EF is considered in the simulated samples equal to the values of 0.001 eV/Å, 0.002 eV/Å, 0.003 eV/Å, 0.005 eV/Å, and 0.01 eV/Å. Fig. 6 shows the variations in the structures in the presence of an EF of 0.01 eV/Å. As can be seen, the structure of the refrigerant oil is not disturbed by the presence of a strongly expressed EF. As a result of the study of EFs described in this section, it can be applied to simulated refrigerant NFs.

Fig. 7 shows the changes in HF in terms of EF applied. According to Fig. 7, the HF created in the structure increases as the EF increases. With the change of EF from 0.001 eV/Å to 0.01 eV/Å, the HF increases by 911 W/m^2 to 942 W/m^2. Physically, the thermal behavior of hydrocast-based NFs improves due to the acceleration of the displacement of atomic samples.

Fig. 8 shows the changes in TC in terms of EF applied. According to Fig. 8, as the EF increases, the amount of TC created in the structure increases. Numerically, by changing the EF from 0.001 eV/Å to 0.01 eV/Å, the TC increases from 0.52 W/m.K to 0.63 W/m.K. This behavior of simulated examples of EF increases oscillation amplitude and can be considered in HT in industrial applications.

Table 3. indicates HF and TC based on the EF applied to the oil hydrocast-based sample after 10 ns. According to Table 3, with the change of EF from 0.001 eV/Å to 0.01 eV/Å, the HF increases from 911 W/m^2 to 942 W/m^2. It also changes the EF from 0.001 eV/Å to 0.01 eV/Å, the TC from 0.52 W/m.K to 0.63 W/m.K.

4. Conclusion

In this work, the thermal behavior of oil inside the nanochannel was investigated by simulating MDS. HF and TC were investigated at temperatures and in the presence of different EFs. The temperatures' values were 310, 320, 330, 350 and 400 K and the magnitude of the EFs was 0.001, 0.002, 0.003, 0.005 and 0.01 eV/Å. The results displayed that:

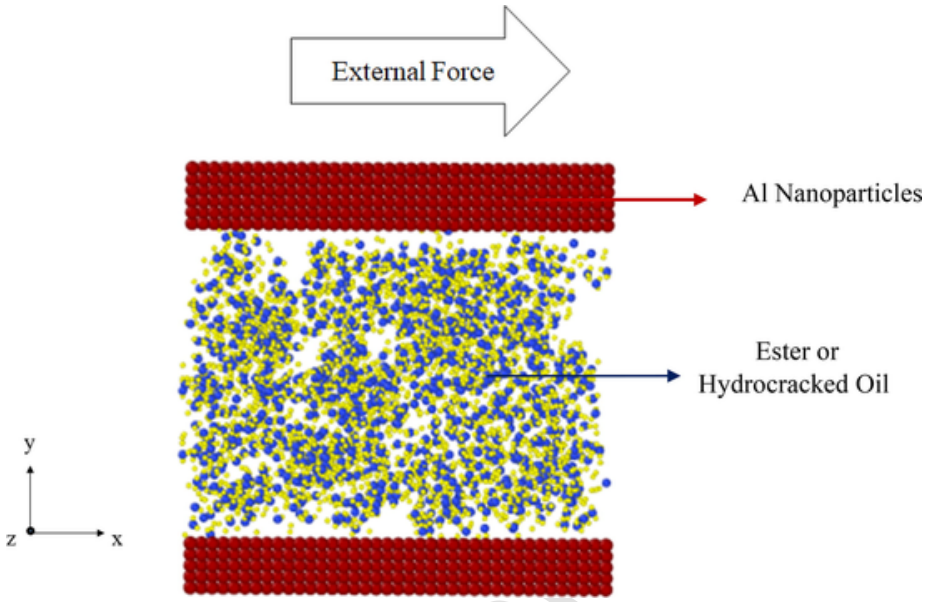

Fig. 6. A schematic of an applied EF in MD simulations.

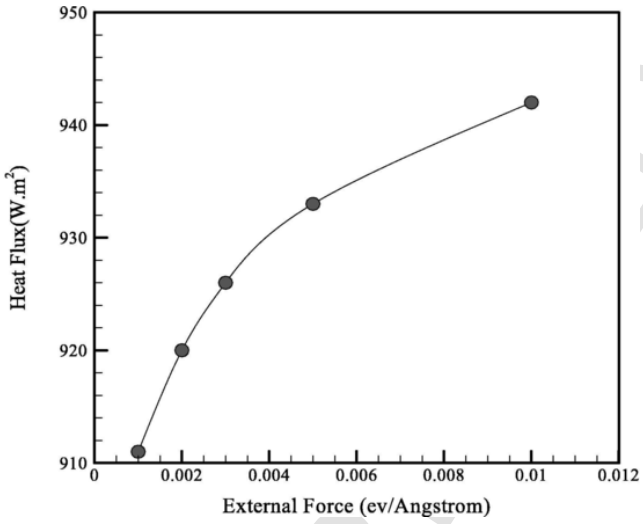

Fig. 7. Changes in oil flux based on hydrocast in EF after 10 ns.

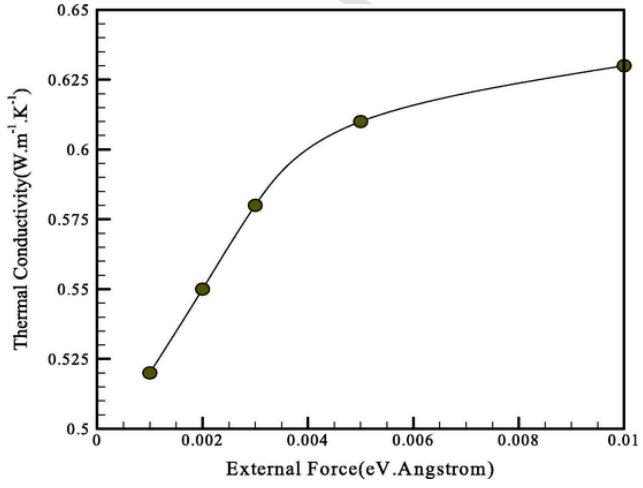

Fig. 8. Changes in oil TC based on hydrocast in EF after 10 ns.

Table 3
HF values and TC based on the EF applied to the oil-based on hydrocast sample after 10 ns.

EF (eV/Å)	TC (W/m.K)	HF (W/m ^{2})
0.001	0.52	911
0.002	0.55	920
0.003	0.58	926
0.005	0.61	933
0.01	0.63	942

- Numerically, the temperature value in the final structure merges to 300 K after 10 ns.
- The PE in atomic structures merges to −1121 eV after 10 ns.
- By enhancing the samples' initial T from 300 to 350 K, the TC value increased from a numerical value of 0.52 to 0.66 W/m.K.
- By expanding the initial T from 300 to 350 K, the HF value increased from a numerical value of 911 to 946 W/m^2.
- Increasing the applied EF from 0.001 to 0.01 eV/Å in the fluid increased the TC value from 0.52 to 0.63 W/m.K after 10 ns.
- By increasing the applied EF from 0.001 to 0.01 eV/Å in the fluid, the HF value increased from a numerical value of 911 to 92 W/m^2 after 10 ns.

CRediT authorship contribution statement

Haoran Cheng : Writing – review & editing, Methodology, Software, Validation. **Azher M. Abed :** Writing – review & editing, Methodology, Software, Validation. **As'ad Alizadeh :** Methodology, Software, Validation. **Amer Ali Ghabra :** Investigation, Writing – review & editing. **Farag M. A. Altalbawy :** Investigation, Writing – review & editing, Methodology, Software, Validation. **Roozbeh Sabetvand :** Investigation, Writing – original draft, Writing – original draft. **Ghassan Fadhil Smaisim :** Investigation, Writing – original draft, Writing – original draft. **Anupam Yadav :** Investigation, Writing – original draft, Writing – original draft. **Davood Toghraie :** Investigation, Writing – original draft, Writing – original draft. **Yassine Riadi :** Investigation, Methodology, Software, Validation.

Declaration of Competing Interest

The authors declare that they have no known competing financial interests or personal relationships that could have appeared to influence the work reported in this paper.

Data availability

No data was used for the research described in the article.

Acknowledgement

National Natural Science Foundation of China (No. 52104028)

References

[1] K. Huang,B. Su, T. Li, H. Ke, M. Lin, et al., Numerical simulation of the mixing behaviour of hot and cold fluids in the rectangular T-junction with/without an impeller, Appl Therm Eng 204 (2022)117942
[2] W. Cui, T. Si, X. Li, X. Li, L. Lu, T. Ma, et al., Heat transfer analysis of phase change material composited with metal foam-fin hybrid structure in inclination container by numerical simulation and artificial neural network, Energy Reports 8 (2022) 10203–10218.
[3] H. Chang, Z. Han, X. Li, T. Ma, Q. Wang, Experimental study on heat transfer performance of sCO2 near pseudo-critical point in airfoil-fin PCHE from viewpoint of average thermal-resistance ratio. International Journal of Heat and Mass Transfer, Int J Heat Mass Tran 196 (2022) 123257.
[4] D, Paliwal, "Experimental Evaluation of Refrigerant Mixtures as Substitutes for HFC134a," *IOSR Journal of Mechanical and Civil Engineering, e-ISSN*, pp. 2278-1684.
[5] S. Benhadid-Dib, A. Benzaoui, Refrigerants and their environmental impact Substitution of hydro chlorofluorocarbon HCFC and HFC hydro fluorocarbon. search for an adequate refrigerant, Energy Procedia 18 (2012) 807–816.
[6] S. Wongwises, N. Chimres, Experimental study of hydrocarbon mixtures to replace HFC-134a in a domestic refrigerator, Energ. Conver. Manage. 46 (1) (2005) 85–100.
[7] J. Tu, C. Qi, Z. Tang, Z. Tian, L. Chen, Experimental study on the influence of bionic channel structure and nanofluids on power generation characteristics of waste heat utilisation equipment, Appl. Therm. Eng. 202 (2022) 117893.
[8] M.Q. Nguyen, M.S. Shadloo, A. Hadjadj, B. Lebon, J. Peixinho, Perturbation threshold and hysteresis associated with the transition to turbulence in sudden expansion pipe flow, Int. J. Heat Fluid Flow 76 (2019) 187–196.
[9] M.S. Shadloo, Application of support vector machines for accurate prediction of convection heat transfer coefficient of nanofluids through circular pipes, Int. J. Numer. Meth. Heat Fluid Flow (2020).
[10] Ieee, Guide for loading mineral-oil-immersed transformers, IEEE Standard 57 (1995) 91–1995.
[11] L.W. Pierce, An investigation of the thermal performance of an oil filled transformer winding, IEEE Trans. Power Delivery 7 (3) (1992) 1347–1358.
[12] H. Nordman, N. Rafsback, D. Susa, Temperature responses to step changes in the load current of power transformers, IEEE Trans. Power Delivery 18 (4) (2003) 1110–1117.
[13] J. Tang, C. Qi, Z. Ding, M. Afrand, Y. Yan, Thermo-hydraulic performance of nanofluids in a bionic heat sink, Int. Commun. Heat Mass Transfer 127 (2021) 105492.
[14] X.M. Lopez-Fernandez, P. Penabad-Duran, J. Turowski, Three-dimensional methodology for the overheating hazard assessment on transformer covers, IEEE Trans. Ind. Appl. 48 (5) (2012) 1549–1555.
[15] J. Tu, C. Qi, K. Li, Z. Tang, Numerical analysis of flow and heat characteristic around micro-ribbed tube in heat exchanger system, Powder Technol. 395 (2022) 562–583.
[16] F. Wang, M.N. Khan, I. Ahmad, H. Ahmad, H. Abu-Zinadah, Y.-M. Chu, Numerical solution of traveling waves in chemical kinetics: Time-fractional fishers equations, Fractals 30 (2) (2022) 2240051.
[17] R. Sadeghi, M.S. Shadloo, M.Y.A. Jamalabadi, A. Karimipour, A three-dimensional lattice Boltzmann model for numerical investigation of bubble growth in pool boiling, Int. Commun. Heat Mass Transfer 79 (2016) 58–66.
[18] H. Nasiri, M.Y. Abdollahzadeh Jamalabadi, R. Sadeghi, M.R. Safaei, T.K. Nguyen, M. Safdari Shadloo, A smoothed particle hydrodynamics approach for numerical simulation of nano-fluid flows, J. Therm. Anal. Calorim. 135 (3) (2019) 1733–1741.
[19] R. Sadeghi, M. Shadloo, Three-dimensional numerical investigation of film boiling by the lattice Boltzmann method, Numerical Heat Transfer, Part A: Applications 71 (5) (2017) 560–574.
[20] M. Ahmadpour, M. Akhavan-Behabadi, B. Sajadi, A. Salehi-Kohestani, Experimental study of R600a/oil/MWCNT nano-refrigerant condensing flow inside micro-fin tubes, Heat Mass Transf. 56 (3) (2020) 749–757.
[21] Y. Feng, J. Hou, D. Wang, S. Wang, H. Hao, D. Shang, J. Wang, Advances in the application of nanofluids molecular dynamics in oil and gas field development, CONVERTER (2021) 269–280.
[22] H. Wang, X. Li, B. Luo, The enhanced heat transfer of diathermic oil-based alumina-doped zinc oxide nanofluids for domestic solar heating systems, J. Therm. Anal. Calorim. 147 (5) (2022) 3977–3988.
[23] L. Wu, B. Song, L.M. Keer, L. Gu, Molecular dynamics investigation of graphene nanoplate diffusion behavior in poly-α-olefin lubricating oil, Crystals 8 (9) (2018) 361.
[24] M.R. Salem, Performance enhancement of a vapor compression refrigeration system using R134a/MWCNT-oil mixture and liquid-suction heat exchanger equipped with twisted tape turbulator, Int. J. Refrig 120 (2020) 357–369.
[25] X. Yong, Modeling the assembly of polymer-grafted nanoparticles at oil-water interfaces, Langmuir 31 (42) (2015) 11458–11469.
[26] J.S. Smith, D. Bedrov, G.D. Smith, A molecular dynamics simulation study of nanoparticle interactions in a model polymer-nanoparticle composite, Compos. Sci. Technol. 63 (11) (2003) 1599–1605.
[27] P.R. Wallace, The band theory of graphite, Phys. Rev. 71 (9) (1947) 622.
[28] H. Berendsen, J. Grigera, T. Straatsma, The missing term in effective pair potentials, J. Phys. Chem. 91 (24) (1987) 6269–6271.
[29] A.K. Rappé, C.J. Casewit, K. Colwell, W.A. Goddard III, W.M. Skiff, UFF, a full periodic table force field for molecular mechanics and molecular dynamics simulations, J. Am. Chem. Soc. 114 (25) (1992) 10024–10035.
[30] M.S. Daw, M.I. Baskes, Embedded-atom method: derivation and application to impurities, surfaces, and other defects in metals, Phys. Rev. B 29 (12) (1984) 6443.
[31] P.G. Huray, Maxwell's equations, John Wiley & Sons, 2011.
[32] M.S. Green, Markoff random processes and the statistical mechanics of time-dependent phenomena. II. irreversible processes in fluids, J. Chem. Phys. 22 (3) (1954) 398–413.